LETTERS
PUBLISHED ONLINE: 2 AUGUST 2009 | DOI: 10.1038/NNANO.2009.194
nature nanotechnology

Structural transformations in graphene studied with high spatial and temporal resolution

Jamie H. Warner[1]*, Mark H. Rümmeli[2], Ling Ge[1], Thomas Gemming[2], Barbara Montanari[3], Nicholas M. Harrison[4], Bernd Büchner[2] and G. Andrew D. Briggs[1]

Graphene has remarkable electronic properties, such as ballistic transport and quantum Hall effects[1–3], and has also been used as a support for samples in high-resolution transmission electron microscopy[4,5] and as a transparent electrode in photovoltaic devices[6]. There is now a demand for techniques that can manipulate the structural and physical properties of graphene, in conjunction with the facility to monitor the changes *in situ* with atomic precision. Here, we show that irradiation with an 80 kV electron beam can selectively remove monolayers in few-layer graphene sheets by means of electron-beam-induced sputtering. Aberration-corrected, low-voltage, high-resolution transmission electron microscopy with sub-ångström resolution is used to examine the structural reconstruction occurring at the single atomic level. We find preferential termination for graphene layers along the zigzag orientation for large hole sizes. The temporal resolution can also be reduced to 80 ms, enabling real-time observation of the reconstruction of carbon atoms during the sputtering process. We also report electron-beam-induced rapid displacement of monolayers, fast elastic distortions and flexible bending at the edges of graphene sheets. These results reveal how energy transfer from the electron beam to few-layer graphene sheets leads to unique structural transformations.

One of the goals of nanotechnology is to be able to manipulate a nanomaterial with atomic precision, while monitoring the rearrangement of the individual atoms in real time as it happens. Electron beam irradiation is an effective tool for the manipulation and modification of carbon nanomaterials, and simultaneously provides a method for *in situ* monitoring using transmission electron microscopy (TEM)[7–12]. High-resolution TEM (HRTEM) characterization of sp^2-based carbon nanomaterials, graphene and single-walled carbon nanotubes (SWNTs) has progressed rapidly in recent years owing to the emergence of aberration-corrected, low-voltage HRTEM[13–15].

The knock-on damage threshold of the hexagonal carbon network in graphite is reported to be 140 keV (ref. 16) and is highly susceptible to structural damage induced by high-angle (that is, $\theta = 180^\circ$) elastic electron–nucleus scattering of electrons with energy above this value. The knock-on damage threshold for carbon atoms is dependent upon the bonding structure of the carbon nanomaterial. In SWNTs and fullerenes, strain is induced in the sp^2 carbon bond due to curvature in the graphene-based structure. This increase in bond strain results in increased chemical reactivity and structural instability compared with the flat sheet of graphene. Saturated carbon atoms in the sp^2 hexagonal lattice of flat sheets of graphene will also behave differently than unsaturated carbon atoms at the edge of the graphene sheets and carbon atoms near defect sites. In the case of graphite the displacement energy is lower for atoms situated within the back surface, and the displacement energy is lower still for unsaturated atoms within the back surface[16] because they have fewer bonds than saturated atoms. Displacement of atoms in the back surface does not require them to be incorporated into the lattice structure; instead, they can be ejected into the vacuum in the direction of momentum transfer from head-on collisions. This results in the loss of material from the back plane and is known as electron beam sputtering.

The interaction of electrons accelerated at 80 kV with graphene and few-layer graphene has received little attention and its effects are relatively unknown[5]. In carbon nanomaterials, electron beam irradiation with energy higher than 80 keV has been used to induce coalescence of fullerenes in SWNT peapods[8], the fusing of two parallel SWNTs in a bundle[6], the formation of junctions between two crossing SWNTs[17] and the phase transformation of carbon 'onions' to diamond[7]. Previous HRTEM studies have demonstrated the capability of resolving the C–C bond and the full lattice structure in graphene and SWNTs, but in these reports long acquisition times (typically 0.5–2 s) were used for producing images[5,12–14]. Thus, the monitoring of motion and structural changes in carbon nanomaterials with fast real-time temporal precision combined with the ability to resolve the atomic structure has been limited. Ultrafast electron microscopy making use of pulsed electron sources has been demonstrated as an approach for obtaining fast temporal resolution[18]; however, the spatial resolution is often not sufficient to resolve the C–C bonds and the atomic structure in carbon nanomaterials.

The maximum energy that can be transferred from an 80 keV electron to a single carbon atom in graphite is $E_{max} = 15.73$ eV (ref. 16). This is well below the displacement energy of saturated non-surface carbon atoms in graphite, which is known to be between 30 and 34 eV (ref. 16). By using electrons accelerated at 80 kV, it is possible that unsaturated carbon atoms will be sputtered from the back surface, giving rise to a preferential loss of carbon atoms surrounding defect sites. Saturated carbon atoms should be robust against knock-on structural damage and remain localized in their position in the graphene lattice. This would require that $E_{us} < 15.73\ \text{eV} < E_s$, where E_{us} and E_s are the respective displacement energies for unsaturated and saturated carbon atoms in the back surface layer.

We have studied the interaction of high-intensity 80 kV electron beam irradiation with few-layer graphene sheets and the resulting sputtering of carbon atoms from a monolayer using *in situ* aberration-corrected HRTEM. TEM examination of the few-layer graphene revealed it was generally composed of between one and six

[1]Department of Materials, Quantum Information Processing Interdisciplinary Research Collaboration, University of Oxford, Parks Road, Oxford OX1 3PH, UK, [2]IFW Dresden, PO Box 270116, D-01171 Dresden, Germany, [3]STFC Rutherford Appleton Laboratory, Didcot, Oxfordshire OX11 0QX, UK, [4]Department of Chemistry, Imperial College, London SW7 2AZ, UK. *e-mail: jamie.warner@materials.ox.ac.uk

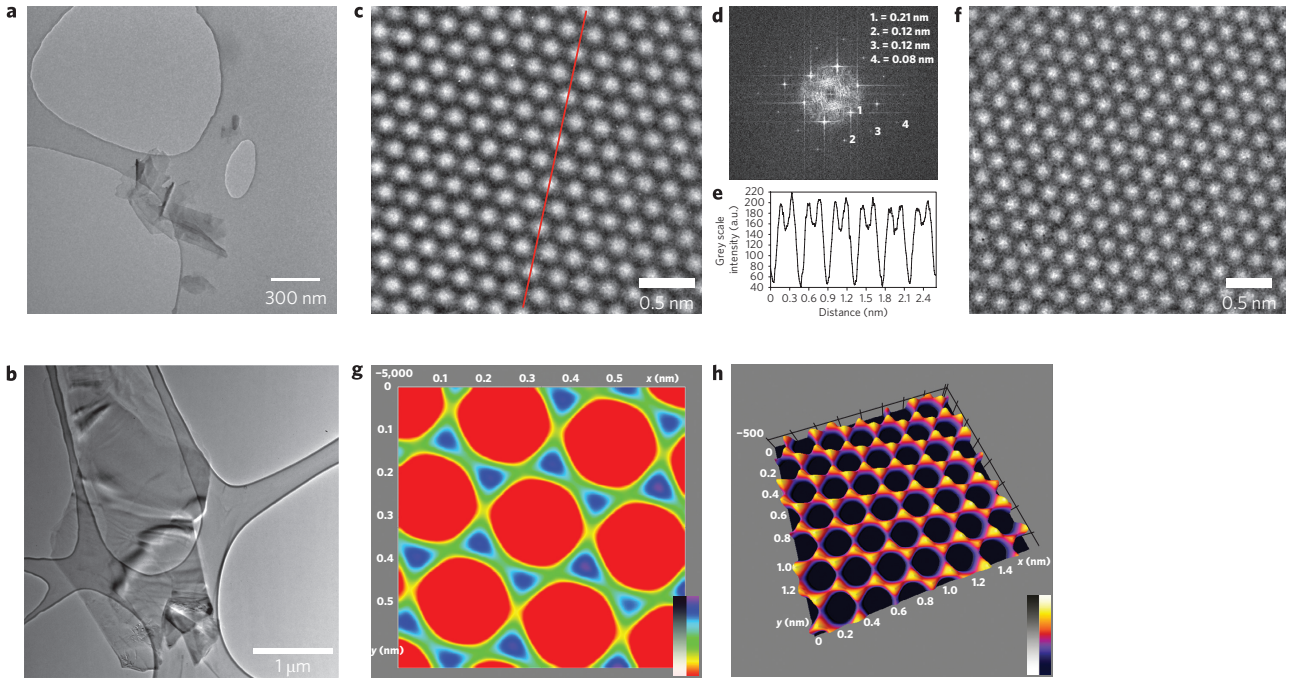

Figure 1 | HRTEM imaging of monolayer and few-layer graphene. a, TEM image of a sheet of few-layer graphene with diameter of 300–500 nm on a lacey carbon-coated grid. **b**, TEM image of a larger sheet of few-layer graphene several micrometres in size. **c**, HRTEM image of a few-layer graphene sheet with five layers. **d**, Two-dimensional FFT taken from **c. e**, Line profile of the grey scale intensity as a function of distance with bright contrast as zero measured along the red line in **c**. Each peak is split into two peaks and demonstrates the ability to resolve the position of individual carbon atoms separated by 1.4 Å. **f**, HRTEM image of a monolayer of graphene. **g**, Reconstructed false-colour image (using *spectrum* false-colour scheme, with the bar indicating mapping of the grey scale to colour) of monolayer graphene showing the individual carbon atoms in the hexagons, generated using an inclusive mask in the FFT that only incorporated the two sets of spots. **h**, Three-dimensional representation of the reconstructed graphene monolayer with contrast used as the *z*-axis (using *fire* false-colour scheme, with the bar indicating mapping of the grey scale to colour).

layers of graphene, which often thinned to monolayer graphene at the edges. The number of graphene layers was determined by analysing the edges of the sheets and counting the layers as holes were formed[14]. Determining the number of layers by fringe counting at the edge can be problematic because of the back-folding of graphene. However, such back-folding results in straight edges that are relatively smooth, like SWNTs. The intrinsic (that is, non-folded) edge of few-layer graphene should have jagged and ragged edges formed during the exfoliation process. Recent work has shown that Joule heating can be used to prepare sharp zigzag and armchair edges in graphitic nanoribbons[19]. We can differentiate edges formed by back-folding and intrinsic edges by their structure under HRTEM. We selected intrinsic edges to conduct our experiments in regions that were free from back-folding. We examined the edges of the sheets between tilt angles of 0° and 30° to determine the number of layers. This correlated well with results obtained by counting the number of layers as they were removed one by one using the electron beam, until a complete hole was formed in the structure.

We examined both few-layer graphene and a monolayer region of graphene. A monolayer of graphene has carbon atoms in a hexagonal arrangement separated by 1.4 Å, whereas few-layer graphene with AB Bernal stacking has a significantly more complex atomic arrangement when tilted with respect to the HRTEM viewing direction and can be used to yield information regarding the imaging resolution. The two-dimensional fast Fourier transform (FFT) taken from Fig. 1c shows sets of distinct spots at 2.1, 1.2, 1.0 and 0.8 Å from the periodic hexagonal structure of AB Bernal stacked few-layer graphene, indicating sub-angstrom resolution at 80 kV. The two-dimensional FFT from the HRTEM of a monolayer showed two sets of spots at 2.1 and 1.2 Å. Individual carbon atoms were resolved in the hexagonal packing arrangement. A three-dimensional representation was formed by plotting the contrast intensity in the *z*-axis, along with the spatial dimensions in the *x*- and *y*-axis, shown in Fig. 1h.

We examined the interaction of electrons accelerated at 80 kV in regions of few-layer graphene by increasing the intensity of the electron beam up to 3 pA nm^{-2}. We found that intense electron beam irradiation resulted in a large number of unsaturated carbon atoms being sputtered from the surface. We found that this process started from an initial vacancy/defect in the lattice structure, and from this site a hole began to grow, rapidly spreading through an entire monolayer. We were not able to determine whether the ejection occurred from the front or back monolayer, but ejection is likely to occur from the back layer based on empirical analogy. Our HRTEM results show a preference for the growth of large holes within the back monolayer rather than the formation of a large number of smaller holes. This indicates that unsaturated carbon atoms are being ejected in preference to saturated carbon atoms within the back surface. Figure 2a–d shows the growth of a hole from an initial vacancy/defect in a graphene bilayer. After 90 s of electron beam irradiation the vacancy has significantly enlarged to a small hole (Fig. 2d). We found that the shape of the hole was continuously changing during the growth period. During the sputtering process multiple atoms may be removed simultaneously from different places around the edge. Once a vacancy loses enough atoms to grow beyond the quad-vacancy state, there are multiple pathways for removing atoms that will lead to different shapes. Thus the stochastic nature of the sputtering process means that the evolution of the pattern of a hole will rarely follow the same pathway. We examined the formation of many holes and found this stochastic nature to be true. Figure 2e–h shows the change in the shape of a hole formed in bilayer graphene. The area of the hole does not change significantly but the direction of the edge termination, and thus

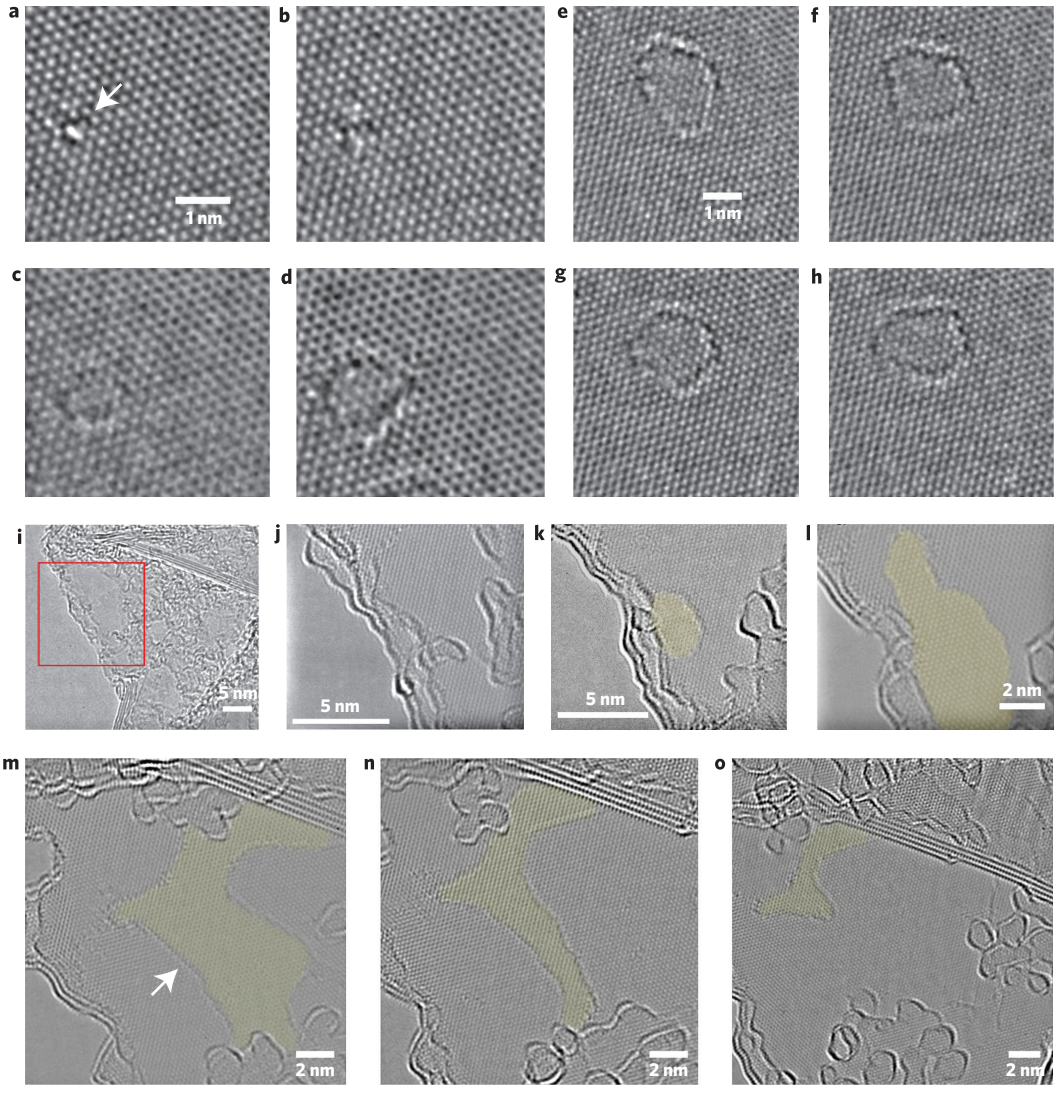

Figure 2 | Selective destruction of graphene monolayer. a–d, Time series of HRTEM images showing the growth of a hole from an initial vacancy/defect in a graphene bilayer, with 30 s between frames. **e–h**, Time series of HRTEM images showing the change in shape of a hole formed in bilayer graphene after an initial period of 2 min of electron beam irradiation with 10 s between frames. **i–o**, Series of images showing the erosion of a monolayer at the edge of a few-layer graphene structure. **i**, TEM image of the edge of few-layer graphene structure. **j–l**, HRTEM images of the edge before intense electron beam irradiation (**j**), and after 2 min (**k**), and 4 min (**l**) of exposure with the hole highlighted in gold. **m–o**, HRTEM images after 6 min (**m**), 8 min (**n**), and 10 min (**o**) of exposure with the remaining monolayer highlighted in gold.

the overall shape and faceting of the hole, changes considerably between each frame.

We performed first-principles calculations using the hybrid exchange density functional B3LYP as implemented in the CRYSTAL package[20] to compare the energy difference between forming two isolated monovacancies and a divacancy in a graphene sheet. This enabled us to determine the difference in energy between removing a carbon atom next to a monovacancy (that is, an unsaturated atom) to create a divacancy and removing another second saturated carbon atom to create two monovacancies. We found that 8.37 eV less energy is required to create one divacancy than two monovacancies, indicating that divacancy formation is the more energetically favourable process. Furthermore, the energy required to remove an unsaturated carbon atom next to a monovacancy to form an isolated carbon atom was determined to be 7.29 eV. This is below the maximum energy of 15.37 eV that can be transferred to single carbon atoms by electrons accelerated at 80 kV and suggests a propensity for sputtering. This supports our *in situ* HRTEM observations that electron beam irradiation at an accelerating voltage of 80 kV preferentially sputters unsaturated carbon atoms surrounding vacancies to form large holes, while fully bonded saturated atoms remain robust against knock-on structural damage.

The sputtering of carbon atoms also occurred at the edges of the few-layer graphene sheets provided there was no back-folding of the graphene sheets. Intrinsic non-folded edges of few-layer graphene sheets contain dangling bonds and unsaturated carbon atoms that are susceptible to sputtering. Figure 2i–o shows a region at the edge of a few-layer graphene sheet exposed to intense electron beam irradiation of up to 3 pA nm^{-2}. After 2 min of exposure a newly formed hole appeared in the back monolayer. The hole increased in size after a further 2 min of electron beam exposure. This was continued for another 6 min, with the remaining portion of the back monolayer highlighted in gold. After the complete removal of this back monolayer we continued the same process and started the selective removal of the next back monolayer. For this layer we concentrated the beam to a smaller area and selected the region exposed in order to remove only half of

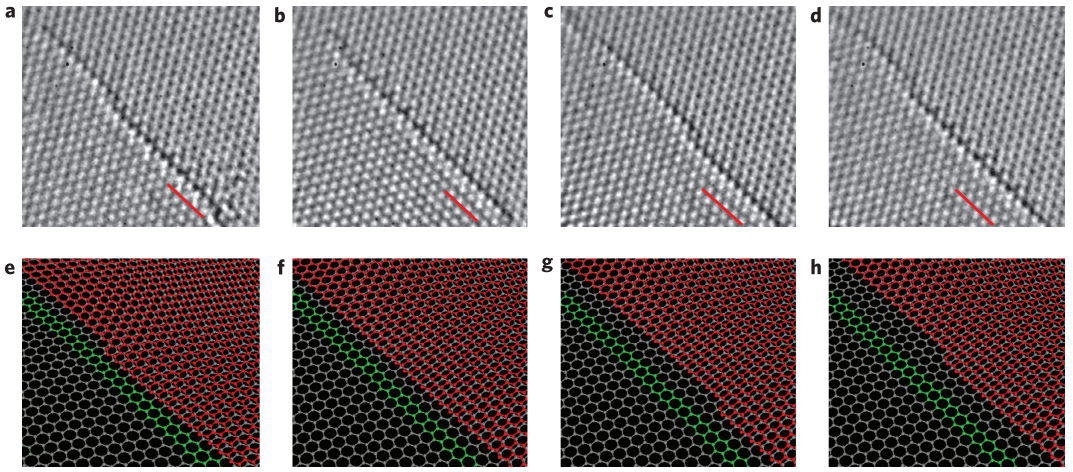

Figure 3 | Zipper-like removal of carbon atoms. Time series of HRTEM images showing the zipper-like removal of carbon atoms along the zigzag edge (Fig. 2e–h). **a–d**, HRTEM images of the straight edge of a large hole in the monolayer at time 0 s (**a**), 2 s (**b**), 4 s (**c**) and 6 s (**d**). **e–h**, Structural representations for each of the HRTEM images presented above.

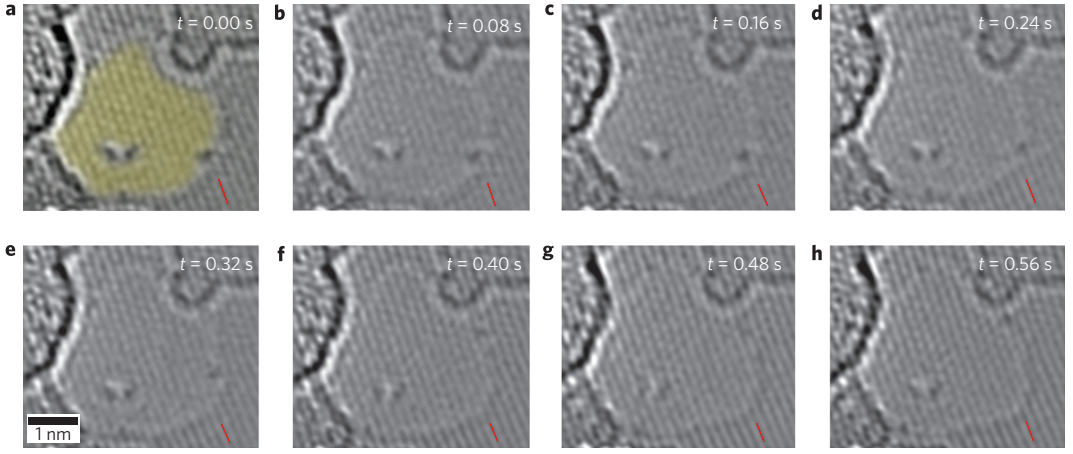

Figure 4 | Stepwise movement of carbon atoms. HRTEM image sequence showing the stepwise movement of carbon atoms around the edge of a graphene monolayer as a function of time during the structural reconfiguration occurring as a result of electron-beam-induced sputtering. The time between each image is 80 ms. A red line has been included in each image in Fig. 4 for reference, allowing changes in positions of atoms to be tracked with high precision.

the monolayer surface area. This enabled us to tailor the back surface of the few-layer graphene to have a monolayer step edge.

The shape of the sputtered holes formed in the back monolayer started out as spherical with some degree of faceting, and as they increased in size the edges straightened out, as indicated with an arrow in Fig. 2m. Figure 3a–d shows the termination of the straight edge of the back monolayer and strong contrast from the edge is seen along the zigzag direction, indicating zigzag termination has higher stability over the armchair configuration. A step in the zigzag row is seen in Fig. 3a and a red line is included as a reference marker to show the loss of carbon along the edge with time. Carbon atoms are lost along the zigzag edge, row by row, and this is attributed to the two carbon atoms at the step between the zigzag rows being unsaturated and susceptible to being sputtered by the electron beam. This results in a zipper-like mechanism for selectively removing one zigzag row of carbon atoms at a time. We found that the zipper mechanism of atomic sputtering only became apparent once the size of a hole had reached a significant size of ~5 nm in diameter.

The structural rearrangement of the edge states of the hole in the monolayer was examined using HRTEM with a fast temporal resolution of 80 ms. We obtained real-time movies (see Supplementary Information) with frame rates of 12 frames per second, lasting up to 15 min, which revealed the behaviour of carbon atoms during the initial stage of the sputtering process. Carbon atoms were often seen moving stepwise around the edges of the monolayer before disappearing. Unlike the carbon atoms recently imaged by others[4], which were adsorbed onto the surface of monolayer graphene, the atoms imaged here are produced at the edges of the bottom layer of graphene due to the sputtering process. We found hardly any carbon adatoms in the central regions of the graphene monolayer, which are far from the edge, confirming that the observed carbon atoms are related to structural reconfiguration at the edge of the sputtered graphene monolayer.

The HRTEM image in Fig. 4a shows a region with a small hole (highlighted in yellow) formed in the bottom layer by electron beam irradiation. A defect (indicated in red) in the bottom monolayer is visible, similar to previous reports[5,12,13]. The defect remains fixed for the duration of this sequence. However, during the course of the entire observation, rearrangement of the carbon atoms surrounding the defect occurs. Strong contrast is observed at the edge of the bottom layer with dimensions no greater than

1–2 carbon atoms and is attributed to an unsaturated carbon atom (indicated with an arrow). From Fig. 4a to d the carbon atom moves along the edge of the monolayer to occupy a position that is slightly higher and also moved to the right to the next row of hexagons. From Fig. 4e to f the carbon atom moves upwards along the edge until it is lost in the top section. This correlates well with the observations presented in Fig. 2e–h, in which the shape of the hole continually changed, demonstrating that structural rearrangement of carbon atoms can occur along the edge during the sputtering process. In most cases we observed that the carbon atoms at the edge of the bottom layer spontaneously disappeared, without a transitional structure of significant high contrast. This indicates that the atoms are being ejected from their position by interaction with the electron beam. Structural reconfiguration of the carbon atoms at the edges of single monolayers of graphene has recently been observed[21].

We also observed several other interesting effects resulting from the interaction of electron beam irradiation with few-layer graphene. We observed rapid switching of defects in few-layer graphene sheets between different stable structural configurations (see Supplementary Fig. S11), captured with a time resolution of 80 ms. Although graphene is reported to be the strongest material ever measured[22], we observed elastic deformations of the graphene sheets, together with significant bending and curling of the sheets at the edges (see Supplementary Figs S12–S14). Enough energy was transferred by the electron beam to overcome van der Waals interactions and drive the motion of pieces of monolayer graphene on the surface of few-layer graphene (see Supplementary Figs S15 and S16). The sliding of a monolayer back and forth on a timescale of 80 ms was observed together with the movement of small pieces across the surface.

In summary, we have shown how aberration-corrected low-voltage HRTEM can be used to examine the interaction between electrons accelerated at 80 kV and few-layer graphene structures with sub-angstrom spatial resolution and 80 ms temporal resolution. The energy delivered to the graphene structures by the electron beam might also, in the future, be used to drive more complex motion, to clean graphene nanodevices, to tailor monolayer–bilayer junctions or, if combined with conductivity measurements, to modify electron transport properties. There may also be the possibility of using electron beam irradiation to provide control over edge termination in graphene monolayers and few-layer graphene after exfoliation, which is known to influence electron transport properties. This concept of *in situ* nanoengineering also paves the way for similar investigations in other sp^2 bonded carbon systems such as SWNTs, fullerenes and carbon nano-peapods.

Methods

Few-layer graphene sheets were prepared by sonicating highly-ordered pyrolytic graphite (HOPG) in 1,2-dichloroethane for 1 h and then centrifuging at 1,000 rpm for 5 min. This removed aggregates, leaving well dispersed few-layer graphene sheets in solution with no signs of aggregation. TEM samples were prepared by dipping a carbon-coated lacey TEM grid into the solution and then removing it. This process allowed the solvent to evaporate quickly and transferred the few-layer graphene onto the grid. The TEM samples were then dried under dynamic vacuum at 100 °C for up to 1–2 h. HRTEM was carried out using an FEI Titan^3 transmission electron microscope with third-order spherical aberration correction, operating at an acceleration voltage of 80 kV, equipped with a charge-coupled device (CCD) (Gatan US1000 2 k × 2 k Camera, 9.5 counts per electrons). Fast temporal resolution was achieved by using 6 pixel binning of the CCD with an overall system magnification of 2.6×10^6. The CCD acquisition time was then reduced to 0.06 s. An electron beam density of up to 3 pA nm^{-2} was used. Camtasia Studio 5 screen recorder software was used to record the live CCD display and produce the movies with 12 frames per second data rate.

Received 8 April 2009; accepted 25 June 2009; published online 2 August 2009

References

1. Du, X., Skachko, I., Barker, A. & Andrei, E. Y. Approaching ballistic transport in suspended graphene. *Nature Nanotech.* **3,** 491–495 (2008).
2. Novoselov, K. S. *et al.* Electric field effect in atomically thin carbon films. *Science* **306,** 666–669 (2004).
3. Novoselov, K. S. *et al.* Two-dimensional gas of massless Dirac fermions in graphene. *Nature* **438,** 197–200 (2005).
4. Meyer, J. C., Girit, C. O., Crommie, M. F. & Zettl, A. Imaging and dynamics of light atoms and molecules on graphene. *Nature* **454,** 319–322 (2008).
5. Meyer, J. C. *et al.* Direct imaging of lattice atoms and topological defects in graphene membranes. *Nano Lett.* **8,** 3582–3586 (2008).
6. Wang, X., Zhi, L. & Mullen, K. Transparent, conductive graphene electrodes for dye-sensitized solar cells. *Nano Lett.* **8,** 323–327 (2008).
7. Terrones, M., Terrones, H., Banhart, F., Charlier, J.-C. & Ajayan, P. M. Coalescence of single-walled carbon nanotubes. *Science* **288,** 1226–1229 (2000).
8. Banhart, F. & Ajayan, P. M. Carbon onions as nanoscopic pressure cells for diamond formation. *Nature* **382,** 433–435 (1996).
9. Hernandez, E. *et al.* Fullerene coalescence in nanopeapods: a path to novel tubular carbon. *Nano Lett.* **3,** 1037–1042 (2003).
10. Warner, J. H. *et al.* Rotating fullerene chains in carbon nanopeapods. *Nano Lett.* **8,** 2328–2335 (2008).
11. Li, J. & Banhart, F. The engineering of hot carbon nanotubes with a focused electron beam. *Nano Lett.* **4,** 1143–1146 (2004).
12. Rodriguez-Manzo, J. A. *et al. In situ* nucleation of carbon nanotubes by the ejection of carbon atoms into metal particles. *Nature Nanotech.* **2,** 307–311 (2007).
13. Hashimoto, A., Suenaga, K., Gloter, A., Urita, K. & Iijima, S. Direct evidence for atomic defects in graphene layers. *Nature* **430,** 870–873 (2004).
14. Suenaga, K. *et al.* Imaging active topological defects in carbon nanotubes. *Nature Nanotech.* **2,** 358–360 (2007).
15. Meyer, J. C. *et al.* The structure of suspended graphene sheets. *Nature* **446,** 60–63 (2007).
16. Egerton, R. F., Li, P. & Malac, M. Radiation damage in the TEM and SEM. *Micron* **35,** 399–409 (2004).
17. Terrones, M. *et al.* Molecular junctions by joining single-walled carbon nanotubes. *Phys. Rev. Lett.* **89,** 0755051 (2002).
18. Park, H. S., Baskin, J. S., Kwon, O.-H. & Zewail, A. H. Atomic-scale imaging in real and energy space developed in ultrafast electron microscopy. *Nano Lett.* **7,** 2545–2551 (2007).
19. Jia, X. *et al.* Controlled formation of sharp zigzag and armchair edges in graphitic nanoribbons. *Science* **323,** 1701–1705 (2009).
20. Dovesi, R. *et al. CRYSTAL06 User's Manual* (University of Torino, 2006).
21. Girit, Ç. Ö. *et al.* Graphene at the edge: stability and dynamics. *Science* **323,** 1705–1708 (2009).
22. Lee, C., Wei, X., Kysar, J. W. & Hone, J. Measurement of the elastic properties and intrinsic strength of monolayer graphene. *Science* **321,** 385–388 (2008).

Acknowledgements

J.H.W. thanks the Violette and Samuel Glasstone Fund and Brasenose College, Oxford, for support. This work was supported in part by the Engineering and Physical Sciences Research Council (EPSRC) through the Quantum Information Processing Interdisciplinary Research Collaboration (GR/S82176/01). G.A.D.B. thanks the EPSRC for a Professorial Research Fellowship (GR/S15808/01). We thank J. H. Jefferson for discussions.

Author contributions

J.H.W. designed and conducted the experiments, analysed the results and wrote the paper. M.R., T.G. and B.B. assisted with the HRTEM measurements. L.G., B.M. and N.M.H. performed the density functional theory (DFT). G.A.D.B. assisted in the analysis of the results.

Additional information

Supplementary information accompanies this paper at www.nature.com/naturenanotechnology. Reprints and permission information is available online at http://npg.nature.com/reprintsandpermissions/. Correspondence and requests for materials should be addressed to J.H.W.